Chapter 5

Luminescence Characteristics of Double Doped $Sr_3Al_2O_6$ Phosphor and Effect of Addition of Flux on $Sr_3Al_2O_6$:R.E.$^{3+}$ System

When you get a result that you expect, you have another result.
When you get a result that you don't expect, you have a discovery.
(Frank Westheimer)

5.1. Introduction

Alkaline earth aluminate (AEA), basically, are oxides of alkaline earth and aluminum ions, which exists in different phases such as binary aluminate, hexaaluminate etc. These binary aluminate/ hexaaluminate compounds became popular from late forties as potent host lattices for fluorescent materials after Froelich [1] first reported photoluminescence from transition ion (Mn^{2+}) activated $SrAl_2O_4$ (binary aluminate) lattice. In 1963 a Belgian [2] described use of rare-earth ions as an activator but a systematic study of $SrAl_2O_4:Eu^{2+}$ was first carried out by Palilla et al. in 1968 [3]. However, until 90's binary alkaline earth aluminate phosphors were less exploited as compared to alkaline earth hexaaluminate phosphors because of relatively longer time of persistence (few seconds) at low brightness level [4]. In mid 1990's Matsuzawa et al. [5] found that introduction of another rare-earth ion, Dy^{3+}, as a co-activator in green emitting $SrAl_2O_4:Eu^{2+}$ system amazingly prolonged the persistence from seconds to many hours, this made it important for many dark vision applications. Since then such co-doping has gained worldwide attention and extensive research work is being carried out on the family of aluminates to synthesize long persistence phosphor with different emission colours.

The addition of the co-dopant in the $Sr_3Al_2O_6:Eu^{2+}$ system is also studied and has a useful application as a mechanoluminscent phosphor [6]. In the last chapter we have seen the energy transfer between Tb^{3+} and Eu^{3+} in $Sr_3Al_2O_6$ system. On the basis of the earlier reports and our last chapter observation, in this chapter we are studying the effect of codopant on the $Sr_3Al_2O_6:Eu^{3+}$ phosphor. The rare earth used for this studies are Samarium, Erbium and Cerium. Also the effect of addition of magnesium in the $Sr_3Al_2O_6:Eu^{3+}$ is also studied.

There have been many investigations, which established that electronic excitation energy could, in certain circumstances, be transferred between ions or molecules in the solid phase. The three basic mechanisms for energy transfer are photoconductive, radiative, and nonradiative [7]. The photoconductive mechanism occurs when an absorbed photon creates free electron-hole pairs capable of migration. Many studies have been conducted on the photoconductivity of semiconductors, and these have generally involved measurement of the electrical current that results after optical excitation. The second basic energy transfer mechanism is radiative reabsorption in which a photon is emitted and then reabsorbed by the same system [7]. This process does not shorten the fluorescence lifetimes, and can usually be minimized by adjusting sample size and

experimental configuration. The mechanism most extensively studied, and most relevant to this thesis, is nonradiative energy transfer between ions without charge migration. In this case Coulomb interactions of the Van der Waals type allow energy to be transferred directly between the ions [8].

Figure 5.1 shows a schematic of the possible luminescence processes which can occur when ion within a larger ensemble is excited.

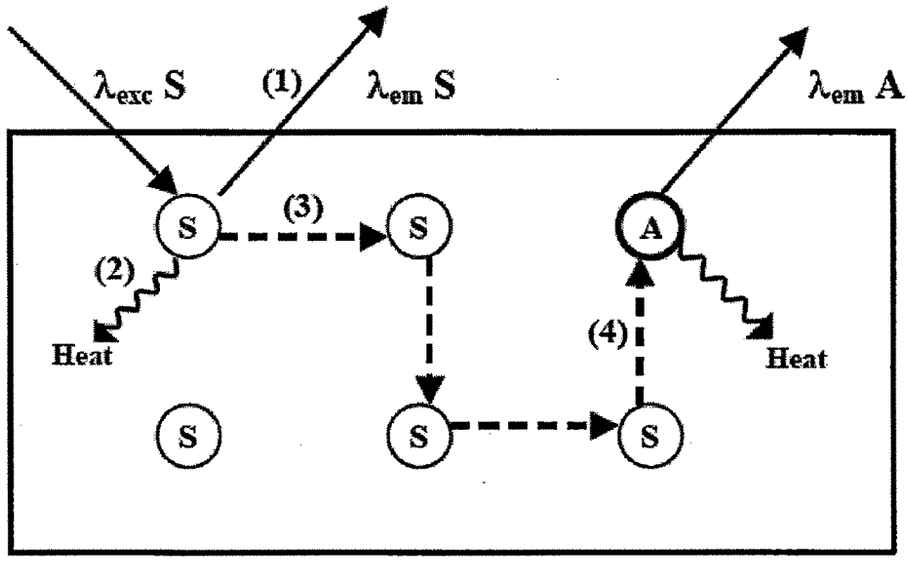

Figure 5.1. Schematic representation of the possible luminescence processes of a crystal system with donor D and acceptor A ions. Following excitation D may: (1) emit radiatively, (2) decay nonradiatively, (3) transfer energy to another D ion,or (4) transfer energy to an A ion. In the last case, energy transfer to A is followed by either radiative or nonradiative decay.

In the host lattice the ion which absorbs the radiation is referred to as the donor, and the ion which excitation energy is transferred is the acceptor. From the schematic presented in Figure 5.1, four different processes following excitation of D can be distinguished:

(1) D may luminescence,

(2) D may decay nonradiatively producing heat,

(3) D may transfer energy to another D type ion, or

(4) D may transfer energy to an A type ion. If energy transfer to A is followed by nonradiative decay, A is referred to as a killer site, because it acts to quench luminescence [9].

In the aluminates system the role of flux addition is very important. The scientists Teng et al [10], Chao-Yeng et al., [11], Kawai et al., [12], Nazarov et al.,[13], Rao et al.,[14], and Harnath et al., [15] has studied the effect of flux on the aluminates.

This chapter conspires the effect of co-dopant as well as the effect of addition of H_3BO_3 as flux on the $Sr_3Al_2O_6$ system.

5.2. Experimental

All the phosphor samples were prepared by the reflux method. The starting materials taken were strontium nitrate, aluminium nitrate and the rare earths in the nitrate form. All of them were acquired from S.D. Fine Chemicals with rare earths of purity 99.9%. The first set of the samples was prepared by doping the Europium nitrate in the host matrix. The powders were weighed according to the nominal composition of $Sr(NO_3)_2$+$Al(NO_3)_3.9H_2O$+ x $R.E.(NO_3)_3$ (x = 0%, 1%, 1.5%, 2%). Second set of samples were prepared with addition of H_3BO_3 as flux with composition as $Sr(NO_3)_2$+$Al(NO_3)_3.9H_2O$+ $R.E.(NO_3)_3$+ y $R.E.(NO_3)_3$ + x H_3BO_3

The starting materials strontium and aluminum nitrates as well as H_3BO_3 were taken in 1:2:10 proportions and dissolved in the appropriate amount of distilled water and kept for stirring. Thereafter the rare earths compounds with different concentrations were mixed to the above solution. Citric acid and ethylene glycol were added to the solution after one hour of constant stirring. The resulting gel was set for refluxing at 100°C for 3 hours. The gel thus obtained, was kept for drying in an oven maintained at 100°C for 10 hours. The yellowish gel then transformed into a fluffy material. It was then kept for firing at a temperature maintained at 900°C in a furnace for 16 hours in air. The white powder obtained on firing, was ground using an agate mortar and pestle and was then subjected to various characterizations.

The photoluminescence (Emission and Excitation spectra) were recorded at room temperature using spectrofluorophotometer RF-5301 PC of SHIMADZU make.

5.3. Results and Discussion

5.3.1. Photoluminescence characteristics of $Sr_3Al_2O_6:Eu^{3+},Ce^{3+}$

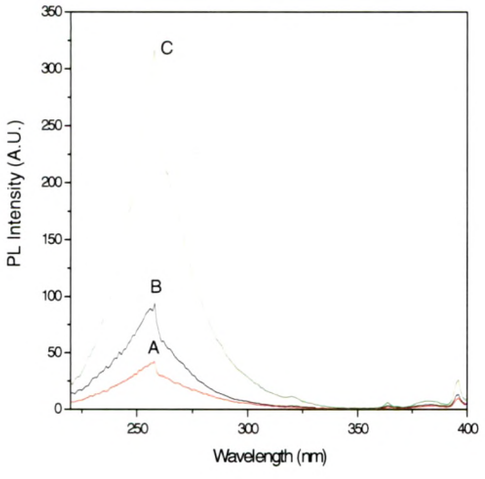

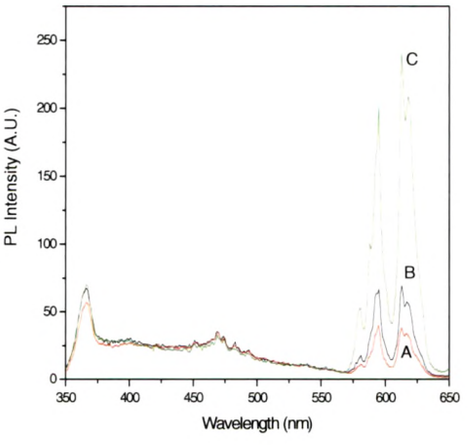

Figure 5.2.A. PL excitation spectra of $Sr_3Al_2O_6$:Eu,Ce with different concentrations of cerium. Emission: 613nm.
Curve A = $Sr_3Al_2O_6$:Eu(1%),Ce(0.1%);
B = $Sr_3Al_2O_6$:Eu(1%),Ce(0.5%);
C =$Sr_3Al_2O_6$:Eu(1%), Ce(1%).

Figure 5.2.B. PL emission spectra of $Sr_3Al_2O_6$:Eu,Ce with different concentrations of cerium. Excitation: 254nm.
Curve A = $Sr_3Al_2O_6$:Eu(1%),Ce(0.1%);
B = $Sr_3Al_2O_6$:Eu(1%),Ce(0.5%);
C =$Sr_3Al_2O_6$:Eu(1%), Ce(1%).

Table 5.1: Summary of PL results of $Sr_3Al_2O_6:Eu^{3+},Ce^{3+}$

Sample Code	Name of the sample	PL emission peak wavelength (nm)	PL Intensity of the peak (A.U.)
A	$Sr_3Al_2O_6$:Eu(1%),Ce(0.1%)	580, 594, 612, 617	10,39,37,33
B	$Sr_3Al_2O_6$:Eu(1%),Ce(0.5%)	580, 594, 612, 617	17,65,69,56
C	$Sr_3Al_2O_6$:Eu(1%),Ce(1%)	580, 594, 612, 617	52,200,240,209

It is well-known that the rare-earth Eu^{2+} and Ce^{3+} ions show the 4f → 5d transitions resulting in a broad band emission in the UV to visible range. Because one electron within the 5d orbit taking part in the formation of chemical bonding (in the excited state), the position of the excitation and emission bands strongly depends on the host lattices, i.e. crystal structure and composition. Therefore, this behaviour allows us to tailor the excitation and emission spectra by varying the dopant and co-dopant and adjusting their concentrations. In this thesis, the Eu^{2+} and Ce^{3+} ions are our firstly chosen as activators and co-activators. The simultaneous incorporation of Eu^{3+} and Ce^{3+} in $Sr_3Al_2O_6$ crystalline

lattice, by the sol gel method, modifies the luminescence spectrum due to the formation of new emission centers.

The energy transfer between Ce^{3+} and Eu^{3+} ions in $Sr_3Al_2O_6$ has, as far as we know, not yet been detected. However this pair is well known for $BaAl_{12}O_{19}:Ce^{3+},Eu^{2+}$ [16], and $Tb_3Al_5O_{12}$:Ce,Eu [17]. From the figure 5.2 A and B, in $Sr_3Al_2O_6:Eu^{3+},Ce^{3+}$, the emission of Ce^{3+} is totally absent in the system. But when acts as co-activator with Eu^{3+} the emission of Eu^{3+} increases. The emission of Eu^{3+} with $^5D_0 \rightarrow {}^7F_{1,2}$ are observed when codoped with Ce^{3+}. The overall intensity of the Eu^{3+} emission increases with increase in the Ce^{3+} concentration as shown in the figure.

The excitation spectra of the $Sr_3Al_2O_6:Eu^{3+}$, Ce^{3+} shows band around 254 nm with the peaks at 490 nm which corresponds to Eu^{3+} transition. The excitation spectra doesn't show any change in the wavelength, except increase in intensity, after addition of the cerium. The excitation spectra was measured upto 400 nm to observe any peaks of Ce^{3+} in the spectra, but no emission / excitation bands of Ce^{3+} has been observed in the spectra.

From the above observation it is clear that the Ce^{3+} acts as sensitizer in $Sr_3Al_2O_6:Eu^{3+}$ system, which helps in improving the luminescence intensity of Eu^{3+}. Ce^{3+} absorbs the UV rays and transfers its energy to Eu^{3+}, where Ce^{3+} is acts as donor and Eu^{3+} as acceptor. The energy gained by the donar to acceptor helps to improve the radiative transitions in this system. The transfer of energy from sensitizer to activator may be accomplished through any of the following mechanism [18]:

(i) emission–reabsorption;

(ii) resonance radiationless;

(iii) non-resonance radiationless.

The radiationless processes indicate that there will not be any emission of sensitizer seen in the emission spectrum. The energy absorbed by the sensitizer is transferred to activator via resonance radiationless process occurring by dipole–dipole or by dipole–quadrupole interaction or via non-resonance radiationless process through exchange interaction [19].

These phosphors were evaluated for possible application in fluorescent lamps, coloured lighting for advertising and flat panel displays.

5.3.2. Photoluminescence of $Sr_3Al_2O_6:Eu^{3+},Mg^{2+}$ Phosphor

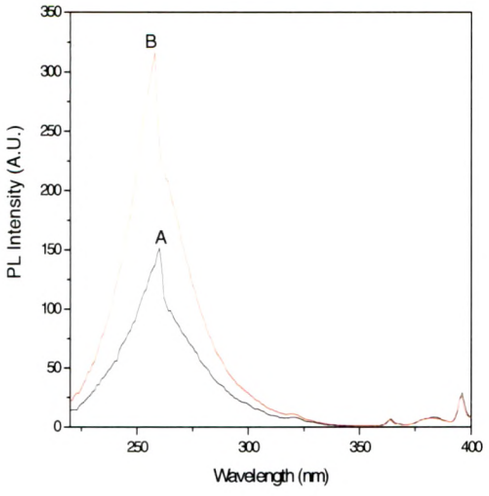

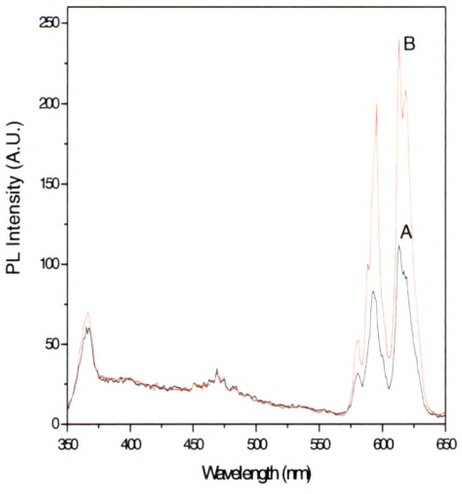

Figure 5.3.A. PL excitation spectra of $Sr_3Al_2O_6$:Eu, Mg. Emission: 613nm. Curve A = $Sr_3Al_2O_6$:Eu(1%),Mg(1%); B = $Sr_3Al_2O_6$:Eu(1%).	**Figure 5.3.B. PL emission spectra of $Sr_3Al_2O_6$:Eu, Mg. Excitation: 254nm. Curve A = $Sr_3Al_2O_6$:Eu(1%),Mg(1%); B = $Sr_3Al_2O_6$:Eu(1%).**

Figure 5.3 A and B represents the excitation and emission spectra of $Sr_3Al_2O_6:Eu^{3+}$, Mg^{2+} phosphor. The Mg^{2+} selected as a co-dopant to see the effect of transition metal on the luminescence study of $Sr_3Al_2O_6:Eu^{3+}$ phosphor. The emission spectra of the phosphor measured for 254 UV excitation shows the emission of Eu^{3+} only and the addition of the Mg^{2+} reduces the intensity of the Eu^{3+} emission. The emission intensity reduces by the factor of 50%. The Mg^{2+} ion acts as luminescence quencher, which reduces the luminescence intensity drastically. As per the theory of energy transfer, here the Mg^{2+} absorbs the excitation energy and transforms that energy into phonon, which reduces the emission of the Eu^{3+} ions in the $Sr_3Al_2O_6$ system.

The excitation spectra measured for 614 nm emission wavelength also shows the band around 254 nm and 390 nm. No other transition is observed in this system. The addition of Mg^{2+} does not affect the excitation band at 490 nm, which resembles to Eu^{3+}.

5.3.3. Photoluminescence of $Sr_3Al_2O_6:Eu^{3+},R.E.^{3+}$

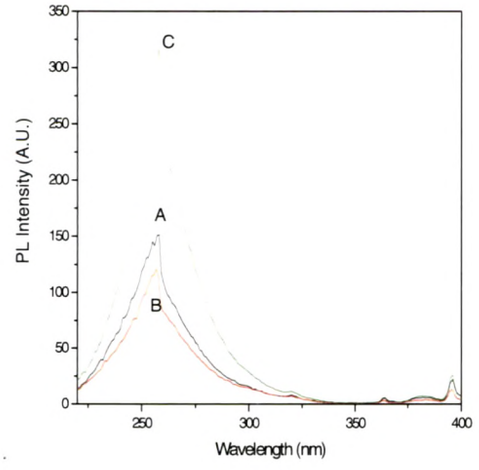

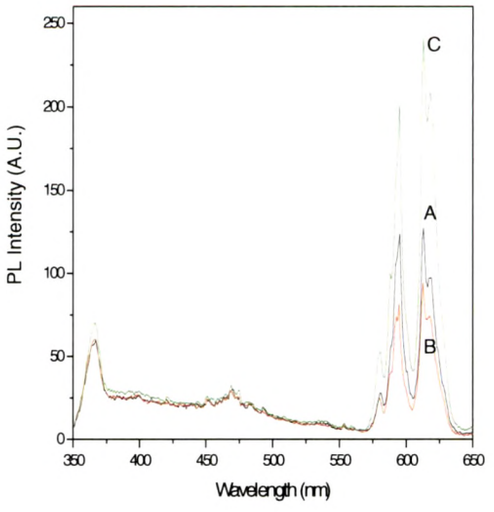

Figure 5.4.A. PL excitation spectra of $Sr_3Al_2O_6$:Eu,R.E. Emission: 613nm. Curve A = $Sr_3Al_2O_6$:Eu(1%),Sm(0.1%); B = $Sr_3Al_2O_6$:Eu(1%),Er(0.1%); C = $Sr_3Al_2O_6$:Eu(1%).

Figure 5.4.B. PL emission spectra of $Sr_3Al_2O_6$:Eu,R.E. Excitation: 254nm. Curve A = $Sr_3Al_2O_6$:Eu(1%),Sm(0.1%); B = $Sr_3Al_2O_6$:Eu(1%),Er(0.1%); C = $Sr_3Al_2O_6$:Eu(1%).

In order to study the different characteristic luminescence of $Sr_3Al_2O_6:Eu^{3+}$ the effect of different co-doping was studied. Figure 5.4. A and B shows the effect of co-doping of Sm^{3+} and Er^{3+} on the PL excitation and emission properties of $Sr_3Al_2O_6:Eu^{3+}$. It is observed from the figure that the addition of Sm^{3+} as well as Er^{3+} reduces the intensity of Eu^{3+} emission. The characteristic emission of Sm^{3+} and Er^{3+} when doped alone in the $Sr_3Al_2O_6$ was not observed. When codoped with the $Sr_3Al_2O_6:Eu^{3+}$ system the excitation energy absorbed by the Sm^{3+} / Er^{3+} ions reduces the emission intensity of Eu^{3+} in this system by more than 50%. The energy levels from which the energy transfer occurs between Sm^{3+}/ Er^{3+} to Eu^{3+} are suppose to be quenching levels.

From the above studies it is observed that there are very few rare earths which helps to enhance red luminescence from Eu^{3+} ion in the $Sr_3Al_2O_6:Eu^{3+}$ system.

Table 5.2: Summary of PL results of $Sr_3Al_2O_6:Eu^{3+},R.E.^{3+}$

Name of the sample	PL emission peak wavelength (nm)	PL Intensity of the peak (A.U.)
$Sr_3Al_2O_6$:Eu(1%),Mg(1%)	580, 592, 613, 617	31,83,110,94
$Sr_3Al_2O_6$:Eu(1%),Sm(0.1%)	580, 594, 612, 617	27,122,125,96
$Sr_3Al_2O_6$:Eu(1%),Er(0.1%)	580, 594, 612, 617	25,79,93,75

5.3.4. Photoluminescence of $Sr_3Al_2O_6:Tb^{3+},Ce^{3+}$ Phosphor

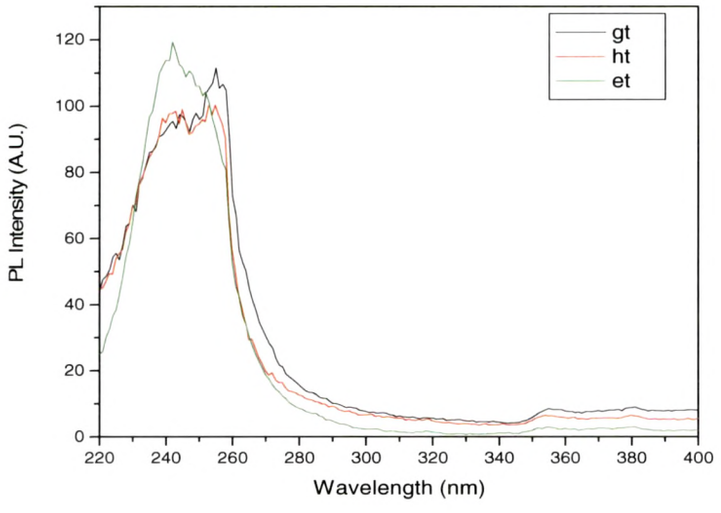

Figure: 5.5. PL excitation spectra of $Sr_3Al_2O_6$:Tb,Ce. Emission: 545 nm.
Curve gt = $Sr_3Al_2O_6$:Tb(0.025%),Ce(0.1%);
ht = $Sr_3Al_2O_6$:Tb(0.025%),Ce(0.05%);
et= $Sr_3Al_2O_6$:TB(0.025%).

The ground state configuration of the Tb^{3+} ion is $4f_8$ and the excited state configuration is $4f_75d_1$, in which the $4f$ shell is half-filled. As the 4f shell is well shielded by the outer electrons within the 5s and 5p orbits, the 4f → 4f transitions of Tb^{3+} are hardly influenced by the environments. Thus, Tb^{3+} shows 4f-4f sharp line emission. Additionally, the $4f_75d_1$ excitation band is normally located at higher energies (< 254 nm), so in order to absorb the 254 nm radiation efficiently, the Ce^{3+} ion is used as a sensitizer through the energy transfer Ce^{3+} →Tb^{3+}. For example in the case of the commercial phosphor $CeMgAl_{10}O_{19}:Tb^{3+}$ (CAT) for use in mercury gas-discharge lamps, by this way Tb^{3+} yields efficient green emission from the $^5D_4$ (to ^7F_J, J = 6 – 0) level [20].

Ce^{3+} has been established as a luminescence sensitizer for the Tb^{3+} ion. The energy transfer process leading to the enhancement of the Tb^{3+} $4f$-$4f$ transition originates from the metastable lowest $5d$ state of the Ce^{3+} ion, and under the proper conditions, the energy transfer rate can be high enough to change the emission dynamics of the donor state.

In the doubly doped system, interionic energy transfer provides an additional competing mechanism for the deexcitation of the Ce^{3+} state.

Figure 5.5 shows the excitation and emission spectra of the $Sr_3Al_2O_6$:Tb^{3+} sample co-doped with Ce^{3+}. The doping concentration of the Tb^{3+} in the phosphor samples was kept as 0.025 mol % for the studies and the concentration of Ce^{3+} was kept as 0.1 mol% and 0.05 mol%, respectively.

The excitation spectra were obtained by monitoring emissions peaks for Tb^{3+} i.e., 545 nm. The excitation curve of $Sr_3Al_2O_6$:Tb^{3+}(0.025%), Ce^{3+}(0.1%) and $Sr_3Al_2O_6$:Tb^{3+}(0.025%), Ce^{3+}(0.05%) shows the peaks around 254nm and 240nm. The excitation spectra of $Sr_3Al_2O_6$:Tb^{3+}(0.025%) shows peak around 254 nm which corresponds to the charge transfer transition of Tb^{3+}. The new band at around 240nm is formed due to incorporation of Ce^{3+} in the phosphor.

The excitation spectrum of the double-doped phosphors seems to contain a significant additional contribution from the Ce^{3+} absorption. Ce^{3+} can strongly absorb UV radiation and efficiently transfer its energy to Tb^{3+}. This process of energy transfer from Ce^{3+} donor to Tb^{3+} acceptor has been observed in many phosphors such as $CaAl_4O_7$:Tb^{3+},Ce^{3+} and for Ce^{3+} in other hosts [21-23].

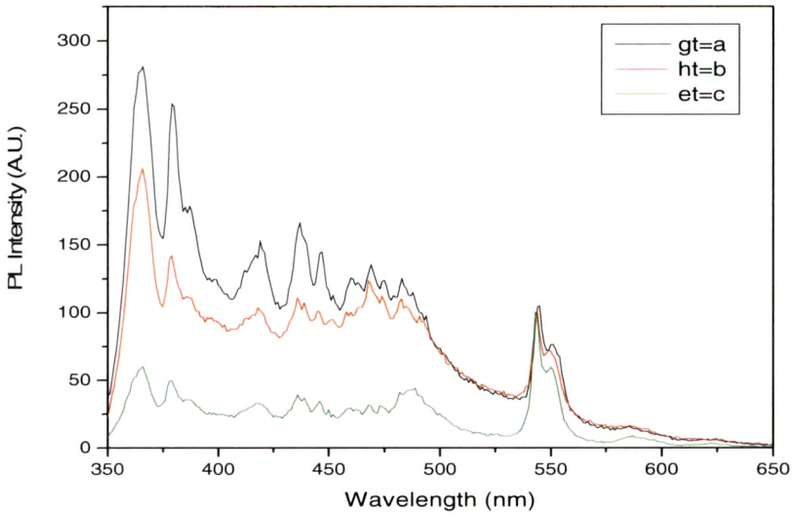

Figure: 5.6. PL emission spectra of $Sr_3Al_2O_6$:Tb,Ce. Emission: 245 nm.
Curve gt = $Sr_3Al_2O_6$:Tb(0.025%),Ce(0.1%);
ht = $Sr_3Al_2O_6$:Tb(0.025%),Ce(0.05%);
et= $Sr_3Al_2O_6$:Tb(0.025%).

The emission spectra of $Sr_3Al_2O_6:Tb^{3+}$(0.025%), $Sr_3Al_2O_6:Tb^{3+}$(0.025%),Ce^{3+}(0.1%) and $Sr_3Al_2O_6:Tb^{3+}$(0.025%), Ce^{3+}(0.05%) are as shown in figure 5.6 when excited with 254 nm wavelength. The curve of $Sr_3Al_2O_6:Tb^{3+}$(0.025%),Ce^{3+}(0.1%) and $Sr_3Al_2O_6:Tb^{3+}$ (0.025%), Ce^{3+}(0.05%) shows the luminescence from $^5D_3$ level of Tb^{3+} along with the $^5D_4$ transitions. Addition of Ce^{3+} into the $Sr_3Al_2O_6:Tb^{3+}$ system increases the intensity of the $^5D_3$ transitions than that of the $^5D_4$ levels. The system shows transitions observed at 365, 379, 418, 437, 447, 460, 470, 475, 482, 545 nm. The emission peaks observed above 400 nm are prescribed to $^5D_3$ to ^7F_J (J = 5,4,3,2,1,0) transitions. Whereas the emission 482 and 545 nm corresponds to $^5D_4$ to ^7F_J (J = 6,5) transition of Tb^{3+}. The presence of emission peaks 365 and 379 was unexpected, also the transitions responsible to this emission are not known as it observed in further studies also. Sharp-line luminescence at -366 nm due to an f-f transition and having a lifetime of milliseconds is observed when the crystal field is weak. We have also measured the emission from 300 nm but no emission from Ce^{3+} was observed. This result shows that Ce^{3+} absorption in the Tb^{3+}–Ce^{3+} system is much stronger than that of Tb^{3+}, because it is a spin and dipole allowed transition. Therefore the energy transfer from Ce^{3+} to Tb^{3+} or Ce^{3+} sensitization effect dominates the energy process. These facts indicate that energy transfer from Ce^{3+} to Tb^{3+} in the co-doped sample may takes place. The enhanced intensity of the $^5D_3$ to ^7F_J transitions of Tb^{3+} in figure 5.6 is very much possible because of the energy transfer process taken place in the

region from 350 to 500nm [24]. The PL emission spectrum doesn't change much when measured for 240 nm excitation except in the reduction in the intensity.

Table 5.3: Summary of PL results of $Sr_3Al_2O_6:Tb^{3+},Ce^{3+}$

Sample Code	Name of the sample	Excitation Peak Wavelength (nm)	PL emission peak wavelength (nm)	PL Intensity of the peak (A.U.)
gt	$Sr_3Al_2O_6$:Tb (0.025%),Ce(0.1%)	245, 254	365,380,419,436, 446,468,482,544	280,254,155,165, 145,137,125,104
ht	$Sr_3Al_2O_6$:Tb(0.025%),Ce(0.05%)	245, 254	365,380,419,436, 446,468,482,544	205,142,102,110, 100,122,110,104
et	$Sr_3Al_2O_6$:Tb(0.025%)	240	365,380,419,436, 446,487,544	60,50,34,38 35,44,104

5.3.5. Thermoluminescence of $Sr_3Al_2O_6:Tb^{3+},Ce^{3+}$ Phosphor

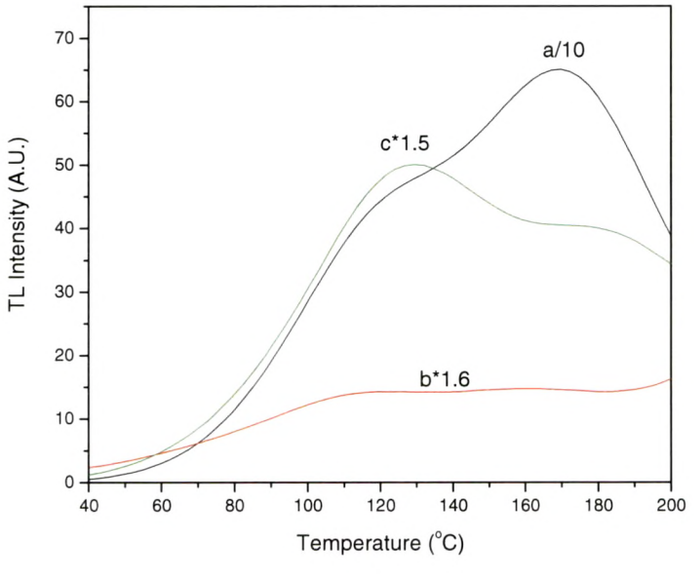

Figure: 5.7. TL glow curve of $Sr_3Al_2O_6$:Tb,Ce. Heating rate = 2 k/s
Curve a = $Sr_3Al_2O_6$:Tb(0.025%),Ce(0.1%);
b= $Sr_3Al_2O_6$:Tb(0.025%),Ce(0.05%);
c = $Sr_3Al_2O_6$:Tb(0.025%).

Figure 5.7 shows the thermoluminescence glow curve of $Sr_3Al_2O_6:Tb^{3+}$(0.025%), Ce^{3+}(0.1%) denoted as 'a' in the curve, $Sr_3Al_2O_6:Tb^{3+}$(0.025%),Ce^{3+}(0.05%) denoted as 'b' in the curve and $Sr_3Al_2O_6:Tb^{3+}$(0.025%) denoted as 'c' in the curve. The above three phosphors were irradiated by beta rays from ^{90}Sr beta source to a dose of 100 Gy. The TL

glow curve was recorded from room temperature to 200 °C for a heating rate of 2 K/s. Above this temperature the kanthal was showing black body radiations, so the peaks beyond 200 °C is suppose to be not reliable. The curve 'c' shows the general order peaks around 124 °C and a hump around 170 °C, which can be isolated by using the T_{stop}-Method, as we have studied this glow curve in the last chapter. This peak was studied as dosimetric peak. The curve 'a' represents the TL glow curve after incorporation of the Ce^{3+}(0.1%) in the $Sr_3Al_2O_6$:Tb^{3+}(0.025%). The addition of Ce^{3+} in the system changes the concentration of the traps. The peak at 124 °C transforms into hump and the hump of the curve 'c' i.e. the peak of 170 °C, now in this case appears as a prominent peak. The intensity of the 170 °C peak increases drastically as shown in the figure, where it is reduced by a factor of 10 for comparison. The increase in the TL intensity of the dosimetric peak is the positive feature of the incorporation of Ce^{3+} as a co-dopant in the $Sr_3Al_2O_6$:Tb^{3+} phosphor. Also the fluorescence emission of the $Sr_3Al_2O_6$:Tb^{3+}(0.025%), Ce^{3+}(0.1%) shows the bluish green emission which has application as a bluish green lamp phosphor. The TL intensity of the 170 °C peak of this phosphor reduces to 20% after 2 months of storage in the dark. This studies indicates that the phosphor $Sr_3Al_2O_6$:Tb^{3+}(0.025%),Ce^{3+}(0.1%) can be used as lamp phosphor as well as dosimetric application.

The TL glow curve of $Sr_3Al_2O_6$:Tb^{3+}(0.025%), Ce^{3+}(0.05%) is as shown as curve 'b' in the figure 5.7. The TL peaks are not defined in this glow curve. The trap is not well separated as well as defined. May be the reason behind such luminescence is the low concentration of the Ce^{3+}(0.05%) in the $Sr_3Al_2O_6$:Tb^{3+} (0.025%) phosphor.

The lower concentration of the Ce^{3+} doesn't help in the formation of traps or may be the formation of trap process is in the intermediate state. Thus the $Sr_3Al_2O_6$:Tb^{3+}(0.025%),Ce^{3+}(0.05%) phosphor cannot be considered as TL / PL phosphor.

5.4. Effect of addition of Flux on the Luminescence Characteristics of $Sr_3Al_2O_6$:R.E.$^{3+}$

In the process of phosphor preparation, some substances are added deliberately to help crystal growth. These substances, which are reactants added deliberately to the raw materials, are called fluxes. Fluxes are usually compounds of alkali-or alkaline earth metals having low melting points. The halides are most frequently used [25]. The flux plays a determining role in the process of particle growth and each flux influences the particle size and shape in a different way. Therefore, a combination of fluxes is sometimes used to obtain products with desired morphology. The selection of flux generally sticks to two principles: one is that the melting point of flux is lower than the reaction temperature; and the other is that impurity ions would not be introduced.

The role of flux materials in the preparation of industrial phosphors is well known. Depending upon the nature of the phosphors, the flux materials are suitably chosen to provide a proper media for an effective incorporation of activating impurities in the system. The effects of boric acid as flux on the sintering process and phosphorescence characteristic were investigated by Chang et al. [26,27] and by Nag and Kutty [28,29]. However, there are no studies about the effect of H_3BO_3 flux on the luminescence and distribution of rare earth ions in $Sr_3Al_2O_6$ phosphors. The addition of flux promotes the pyrolysis of strontium based starting materials [30]. Furthermore, it can replace the Al^{3+} and lead to distortions due to its low ionic radius compared to Al^{3+} [31]. These two factors result in the growth of the host crystals.

The synthesis of $Sr_3Al_2O_6:Eu^{2+}$ by addition of H_3BO_3 as a flux is mentioned by Morito Akiyama et al [32]. They have reported in the increase in the PL intensity along with the single phase formation after using flux in the system.

When the phosphor is doped with H_3BO_3 as flux, parts of B entering crystal lattice replace Al. However, large parts of B do not enter crystal lattice, which melt at low temperature and act as flux for the synthesis of the phosphor. It is suitable for producing pure phase and easy to hold integrality of crystal due to the low melting point of the compound. B which does not enter crystal lattice is help to urge activator ions entering crystal lattice and form single phase $Sr_3Al_2O_6$:R.E.$^{3+}$.

The effects of boron addition on the luminescence properties of the $Sr_3Al_2O_6$:R.E.$^{3+}$, synthesized via a reflux sol-gel route, was systematically investigated.

5.4.1. Photoluminescence of $Sr_3Al_2O_6$:Eu^{3+},H_3BO_3

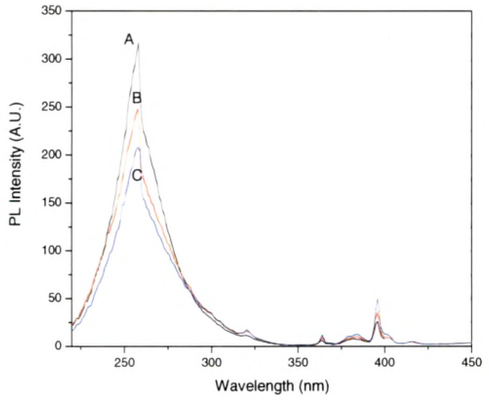

Figure: 5.8.A. PL excitation spectra of $Sr_3Al_2O_6$:Eu,H_3BO_3. Emission: 613nm. Curve A = $Sr_3Al_2O_6$:Eu(1%); B = $Sr_3Al_2O_6$:Eu(1%), H_3BO_3 (10%); C = $Sr_3Al_2O_6$:Eu(1%), H_3BO_3 (20%).

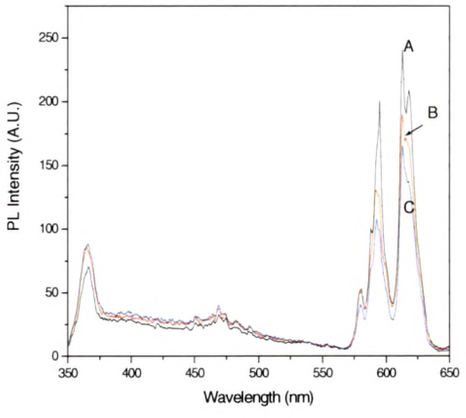

Figure: 5.8.B. PL emission spectra of $Sr_3Al_2O_6$:Eu, H_3BO_3. Excitation: 254nm. Curve A = $Sr_3Al_2O_6$:Eu(1%); B = $Sr_3Al_2O_6$:Eu(1%), H_3BO_3 (10%); C = $Sr_3Al_2O_6$:Eu(1%), H_3BO_3 (20%).

The figure 5.8 A and B represents the effect of addition of flux on the fluorescence characteristics of $Sr_3Al_2O_6$:Eu^{3+} system. The excitation and emission spectra were measured for 613nm and 254nm respectively. Curve 'A' represents the excitation/emission spectrum of $Sr_3Al_2O_6$:Eu^{3+}(1%), where as curve 'B' and curve 'C' represents the spectra of $Sr_3Al_2O_6$:Eu^{3+}(1%), H_3BO_3(10%) and $Sr_3Al_2O_6$:Eu^{3+}(1%), H_3BO_3(20%). The excitation curve shows that there is fall in the intensity of the excitation spectra when flux is added in the system. But intensity of the excitation transitions of Eu^{3+} i.e., the peaks around 365 and 395 nm increase slightly after addition of the flux. Sharp-line luminescence at -366 nm due to an f-f transition and having a lifetime of milliseconds is observed when the crystal field is weak, as we have already discussed in Section 5.3.4. The PL emission spectra shows that on addition of the flux in the system, the intensity of the Eu^{3+} emission reduces by around 20% when the concentration of H_3BO_3 is 10 mol% with respect to the stoichiometric of $Sr_3Al_2O_6$. Increasing the flux concentration to 20 mol% reduces the PL emission intensity by another 20%. The reason behind this is may be the host of boron-modified $Sr_3Al_2O_6$ consists of a nonhomogeneous composite that includes mostly $Sr_3Al_2O_6$ and a minor

proportion of glassy strontium borates formed from SrO and B_2O_3. Pei *et al.*[33] proposed a substitution defect model that states nonequivalent substitution of Eu^{3+} for Sr^{2+} creates electrons on Sr^{2+} vacancies in strontium borates. The anionic BO_4 tetrahedra of metal borates were believed to play an important role of electron transfer in the reduction process of Eu^{3+} to Eu^{2+}, and the network of BO_4 tetrahedra may also act as a shield to prevent oxygen diffusion. Consequently, boron addition in the synthesis of $Sr_3Al_2O_6$ in fact favors the conversion of Eu^{3+} into Eu^{2+}. The luminescence from the Eu^{2+} is totally get quenched in $Sr_3Al_2O_6$ system, hence the emission intensity get reduced on the addition of flux. On addition of flux, the presence of both Eu^{2+} and Eu^{3+} states in the $SrAl_2O_4$ system has also been observed by Zhang et al. [34].

Table 5.4: Summary of PL results of $Sr_3Al_2O_6:Eu^{3+},Dy^{3+}$, H_3BO_3

Sample Code	Name of the sample	Excitation Peak Wavelength (nm)	PL emission peak wavelength (nm)	PL Intensity of the peak (A.U.)
A	$Sr_3Al_2O_6$:Eu(1%)	257,363,381,395	580,54,612,618	53,201,240,208
B	$Sr_3Al_2O_6$: Eu(1%),H_3BO_3(10%)	257,363,381,395	580,54,612,618	53,132,190,172
C	$Sr_3Al_2O_6$: Eu(1%),H_3BO_3(20%)	257,363,381,395	580,54,612,618	38,105,164,135
D	$Sr_3Al_2O_6$: Eu(1%),Dy(0.1%)H_3BO_3(10%)	257,363,381,395	580,54,612,618	30,90,128,102

5.4.2. Photoluminescence of $Sr_3Al_2O_6:Eu^{3+}$, Dy^{3+}, H_3BO_3

The studies of aluminate system mainly have focused on doping with the second activator except Eu^{2+} since 1990s, such as Dy^{3+}, Nd^{3+}, etc. It is hoped that the phosphor can form the proper trap energy level via doping microelement, thereby achieve the aim that enhance luminescent brightness and prolong afterglow time [35-37]. At the same time, the effect of flux on synthetic techniques and luminescent properties has become one of the hotspot in the aluminate luminescent materials activated by rare earth [38-40]. Chen et al. [41] studied the effect of B_2O_3 on the properties of $SrAl_2O_4:Eu^{2+}$, Dy^{3+} prepared by sol–gel method. The figure 5.9 A and B shows the PL excitation and emission spectra of $Sr_3Al_2O_6:Eu^{3+}$(1%),Dy^{3+}(0.1%) with and without flux. The concentration of H_3BO_3 is 10%. The position of the emission peak does not change when the phosphor is doped with H_3BO_3 as flux, which shows the emission due to Eu^{3+}. But the emission intensity of the phosphor prepared with H_3BO_3 is reduced than that of the phosphor prepared without H_3BO_3. The reason behind the reduction in the intensity is may be due to the transformation of Eu^{3+} into Eu^{2+} state.

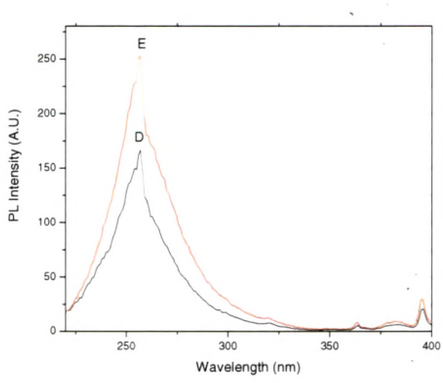

Figure: 5.9.A. PL excitation spectra of $Sr_3Al_2O_6$:Eu, Dy, H_3BO_3. Emission: 613nm.
Curve D = $Sr_3Al_2O_6$:Eu(1%), Dy(0.1%), H_3BO_3 (10%); E = $Sr_3Al_2O_6$:Eu(1%), Dy(0.1%).

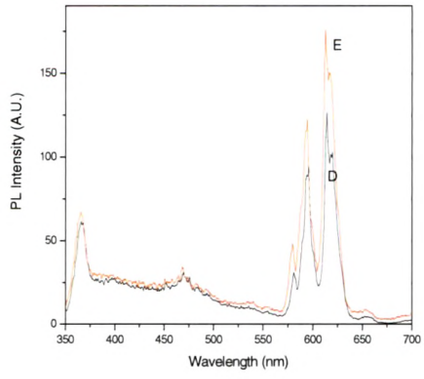

Figure: 5.9.B. PL emission spectra of $Sr_3Al_2O_6$:Eu, Dy, H_3BO_3. Excitation: 254nm.
Curve D = $Sr_3Al_2O_6$:Eu(1%), Dy(0.1%), H_3BO_3 (10%); E = $Sr_3Al_2O_6$:Eu(1%), Dy(0.1%).

5.4.3. Photoluminescence of $Sr_3Al_2O_6$:Tb, R.E., H_3BO_3

Figure 5.10 A and B shows the PL excitation and emission spectra of $Sr_3Al_2O_6:Tb^{3+}$(0.03%), $Sr_3Al_2O_6:Tb^{3+}$ (0.03%), H_3BO_3 (3%) and $Sr_3Al_2O_6:Tb^{3+}$ (0.03%), H_3BO_3 (20%), denoted as curve 'A', 'B' and 'C', respectively. The excitation spectra of curve 'A' shows the peak around 240 nm which is attributed to the charge transfer transition of Tb^{3+} in the $Sr_3Al_2O_6$ system. Whereas, the curve 'B', the flux was added, shows the peak around 254 nm having a hump around 240 nm wavelengths. There is a drastic change in the excitation spectrum of 3 mol% flux added system. Curve 'C' shows the excitation spectrum of 20 mol% added flux, where again the prominent peak appears around 240 nm and a hump around 254 nm is observed. This fact suggests that at lower concentration of flux addition, the crystal field surroundings of Tb^{3+} are changed due to the incorporation of BO_3 in the lattice.

The PL emission spectra are as shown in the figure 5.9.B. After introducing flux (3 mol%) into the $Sr_3Al_2O_6:Tb^{3+}$ system, the relative PL intensity of 545 nm peak increases by 40%. Also the multiple peaks at 420, 437, 447, 460, 483 and 488 nm were observed which corresponds to the $^5D_3$ and $^5D_4$ transitions of Tb^{3+}. Hence, the addition of lower concentration of flux is responsible for the emission in violet, blue and green region of the visible spectrum. The combination of all these colors resulted into the white light emission.

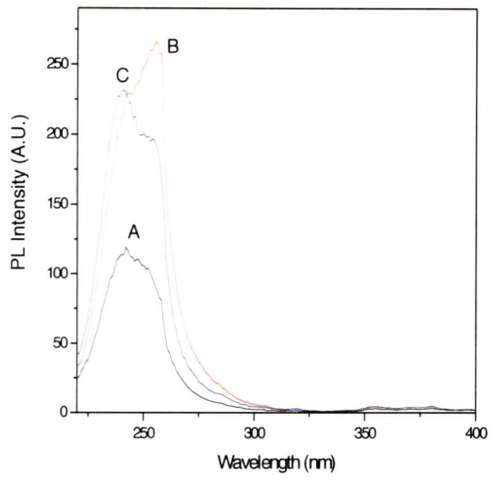

Figure: 5.10.A. PL excitation spectra of $Sr_3Al_2O_6$:Tb, H_3BO_3. Emission: 545nm. Curve A = $Sr_3Al_2O_6$:Tb(0.03%); B = $Sr_3Al_2O_6$:Tb(0.03%), H_3BO_3(3%); C= $Sr_3Al_2O_6$:Tb(0.03%), H_3BO_3(20%).

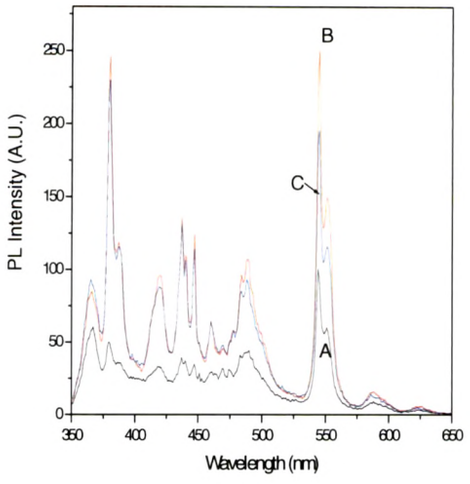

Figure: 5.10.B. PL emission spectra of $Sr_3Al_2O_6$:Tb,H_3BO_3. Excitation: 254nm. Curve A = $Sr_3Al_2O_6$:Tb(0.03%); B = $Sr_3Al_2O_6$:Tb(0.03%), H_3BO_3 (3%); = $Sr_3Al_2O_6$:Tb(0.03%), H_3BO_3 (20%).

In the lower (<10 mol%) concentration range, H_3BO_3 acted as a better fluxing agent in promoting formation of the required crystalline phase for producing efficient luminescent characteristics, whereas in the higher (~ 20 mol%) range it behaved as one of the precursor materials for formation of aluminoborate complexes, which in turn cloaked the luminescence. Our results strongly accentuate the idea that the addition of an optimum amount of H_3BO_3 greatly increases the energy conversion efficiency of the phosphor.

Initially it was thought the boric acid promotes only crystallization and acts as a high temperature solvent because it has good solubility with the oxide materials used. But during this study we found that H_3BO_3 not only reduces the processing temperatures but also strongly influences the phase stabilization and luminescence centre formation [28]. If the crystallization is done properly, it is the flux that facilitates the entry of the activator into the crystal lattice and aids in the formation of a luminescent centre [42]. In the higher concentration of boric acid addition, the borate ions participate in the formation of superstructure units by the breaking of O–Al–O to form O–Al–B bonds [40]. More often, phases other than $Sr_3Al_2O_6$ tend to contribute more of non-radiative transitions, which in turn decrease the overall PL intensity of the phosphor.

Table 5.5: Summary of PL results of $Sr_3Al_2O_6:Tb^{3+},Ce^{3+},H_3BO_3$

Sample Code	Name of the sample	Excitation Peak Wavelength (nm)	PL emission peak wavelength (nm)	PL Intensity of the peak (A.U.)
A	$Sr_3Al_2O_6$:Tb (0.03%)	240	365,380,420,437,446, 487,544,550,586	58,50,32,37, 34,42,99,59,8,6
B	$Sr_3Al_2O_6$:Tb(0.03%), H_3BO_3(3%)	240,254	365,380,420,437,446, 460,487,544,550,586	83,245,94,134, 123, 64,107,250,551 ,14,6
C	$Sr_3Al_2O_6$:Tb(0.03%), H_3BO_3(20%)	240,254	365,380,420,437,446, 460,487,544,550,586	93,228,88,133, 122, 62,92,193,115, 12,6
Y	$Sr_3Al_2O_6$:Tb(0.03%),Ce(0.1%) H_3BO_3(3%)	254	365,380,420,437,446, 460,487,544,550,586	81,138,63,85,7 8,48,51,65,43,5 ,2

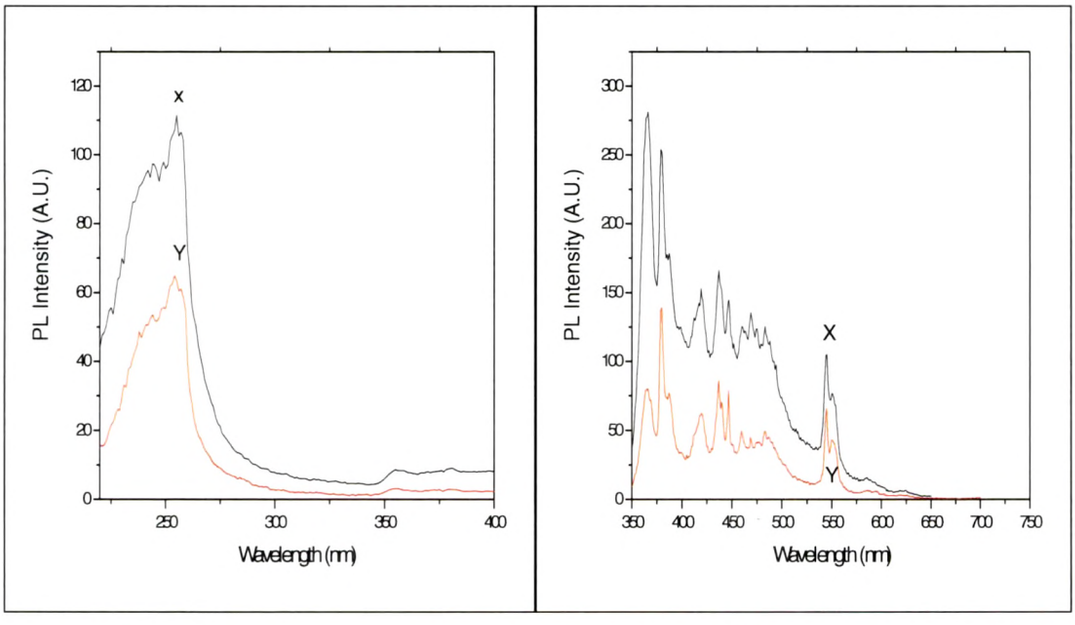

Figure: 5.11.A. PL excitation spectra of $Sr_3Al_2O_6$:Tb,Ce,H_3BO_3. Emission: 545nm. Curve X = $Sr_3Al_2O_6$:Tb(0.025%),Ce(0.1%); Y= $Sr_3Al_2O_6$:Tb(0.025%), Ce (0.1%), H_3BO_3 (3%).

Figure: 5.11.B. PL emission spectra of $Sr_3Al_2O_6$:Tb,Ce,H_3BO_3. Excitation: 254nm. Curve X = $r_3Al_2O_6$:Tb(0.025%),Ce(0.1%); Y= $Sr_3Al_2O_6$:Tb(0.025%), Ce (0.1%), H_3BO_3 (3%).

Figure 5.11 A and B shows the excitation and emission spectra of $Sr_3Al_2O_6:Tb^{3+}$(0.025%), Ce^{3+}(0.1%) and $Sr_3Al_2O_6:Tb^{3+}$(0.025%), Ce^{3+}(0.1%), H_3BO_3 (3%) system, denoted as curve 'X' and 'Y', respectively.

The excitation as well as emission spectra shows the reduction in the intensity by 40% after addition of flux in the system. The peak shift was not observed in the excitation as well as emission spectra after the flux introduction, which represents that there is no change in the crystal field symmetry due to BO_3.

The emission spectrum of $Sr_3Al_2O_6:Tb^{3+},Ce^{3+}$ without any flux shows the peaks from 360 to 560 nm where we are not able to verify the origin of the 360 and 380 nm peaks. All the other peaks are observed due to the transition of Tb^{3+} in the $^5D_3$ and $^5D_4$ state.

The addition of flux reduces the PL emission intensity of all the peaks in the spectra. May be in the double dopant system, reacts with SrO and/or Al_2O_3 to form a layer of amorphous strontium aluminoborate grain boundary phase on the surface of the $Sr_3Al_2O_6$ grain and most of the rare earth Tb^{3+} and Ce^{3+} deposit in the grain boundary phase. Only small amounts of Tb^{3+}, Ce^{3+} can go into the $Sr_3Al_2O_6$ lattice.

Though the resultant $Sr_3Al_2O_6$ is single phase, the luminescence properties of $Sr_3Al_2O_6:Tb^{3+},Ce^{3+}$ is poor.

5.5. Low Temperature TL of $Sr_3Al_2O_6:Eu^{3+}$ (1%), X^{3+} phosphors

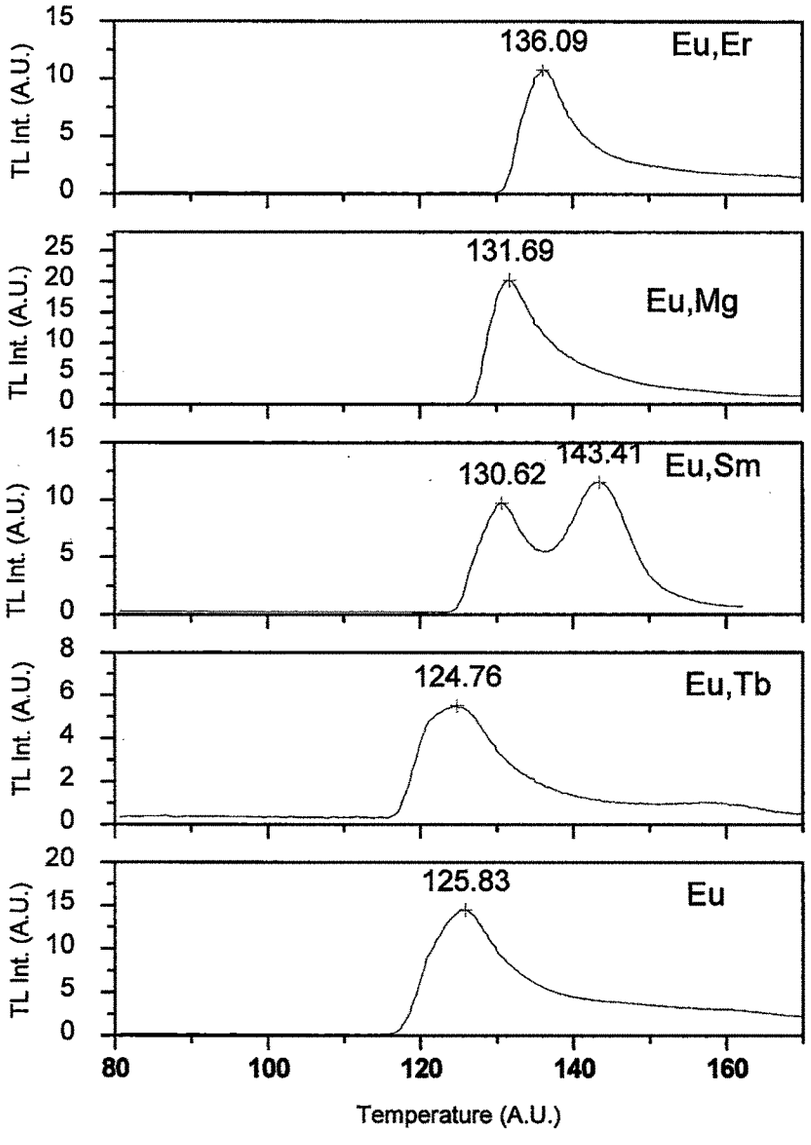

Figure: 5.12. TL glow curve of $Sr_3Al_2O_6$:Eu,R.E. Heating rate = 2 k/s
Curve Eu = $Sr_3Al_2O_6$:Eu(1%);
Eu,Tb= $Sr_3Al_2O_6$:Eu(1%),Tb(0.1%);
Eu,Sm= $Sr_3Al_2O_6$:Eu(1%),Sm(0.1%);
Eu,Mg= $Sr_3Al_2O_6$:Eu(1%),Mg(1%);
Eu,Er = $Sr_3Al_2O_6$:Eu(1%),Er(0.1%).

Table 5.6: Summary of TL results of $Sr_3Al_2O_6:Eu^{3+}$,R.E.$^{3+}$

Sample Code	Name of the sample	TL Peak Temperature (°C)	TL peak Intensity (A.U.)
Eu	$Sr_3Al_2O_6$:Eu(1%)	125.83	15
Eu,TB	$Sr_3Al_2O_6$:Eu(1%),Tb(0.1%)	124.76	5
Eu,Sm	$Sr_3Al_2O_6$:Eu(1%),Sm(0.1%)	130.62, 143.41	10, 12
Eu,Mg	$Sr_3Al_2O_6$:Eu(1%),Mg(1%)	131.69	21
Eu,Er	$Sr_3Al_2O_6$:Eu(1%),Er(0.1%)	136.09	11

Figure 5.12 shows the characteristics of $Sr_3Al_2O_6:Eu^{3+}$, X^{3+} system where X = Sm^{3+},Tb^{3+}, Mg^{3+},Er^{3+} have been studied in the temperature region -180 to -70°C. Thermoluminescence (TL) is one of the most useful methods to study the trapping levels in materials. The measurement of the TL glow curves should thus reveal new facts about the luminescence mechanisms of double-doped phosphors.

The thermoluminescence characteristics of $Sr_3Al_2O_6:Eu^{3+}$, $Sr_3Al_2O_6:Eu^{3+}$,Sm^{3+}, $Sr_3Al_2O_6:Eu^{3+}$,Tb^{3+}, $Sr_3Al_2O_6:Eu^{3+}$,Mg^{3+} and $Sr_3Al_2O_6:Eu^{3+}$,Er^{3+} were measured at low temperature to find out whether there is any peak near the room temperature which can be responsible for the phosphorescence. It is observed that changing the co- dopant to the adjacent element (i.e., Eu^{3+}) in the lanthanide series affects significantly the thermoluminescence intensity and even the position of the glow curve maximum. The low temperature TL studies of this phosphor is also been published [43]

The Yun Liu et al., [44] have also measured the low temperature TL of the SrO-Al_2O_3 system doped with Eu^{2+} in which they studied the compounds fired at different temperatures viz. 750, 1000, 1300 and 1400 °C; the phosphor fired in the temperature regime 750-1000 °C shows the presence of $Sr_3Al_2O_6$ as well as $SrAl_2O_4$ phase. They observed from the photoluminescence studies that the europium resides in the SAO system in the Eu^{3+} as well as Eu^{2+} valence states in the matrix when fired from 750 to 1000 °C. The low temperature TL of this phosphor measured between –50 to 250 °C shows that the defects were found to form a continual trap energy level. The coexisting Eu^{3+} ions decreased the efficient emission centers from the Eu^{2+} ions and drop down the emission intensity. This continual trap level was separated into the two-overlapped trap energy levels for temperature treatment at 1300 °C.

The low temperature TL glow curves were recorded in the laboratory of Prof. Louis Rey , AREAL Crt, Illkrish, France. For measuring low temperature TL, the phosphor weighing

1mg were taken in aluminum cavities and the samples were cooled to liquid nitrogen and are irradiated using Philips X-ray irradiator. Prior to irradiation the samples were placed in aluminum test cavities of 20mm diameter and 2mm depth and frozen to –20 °C on a cold metallic block. The frozen samples were finally immersed into liquid nitrogen for one hour. A test dose of 0.5kGy X-ray is imparted to the specimens, maintained at -196°C. The irradiated samples were then immediately transferred to low temperature thermoluminescence equipment which is maintained at -196°C and recorded TL. Heating rate used for measuring TL is 5°C/minute.

The phosphors were subjected to the Thermally Stimulated Luminescence (TSL) study to ascertain the defects present in the synthesized compounds. Figure 5.12 represents the TL exhibited by the phosphors at low temperatures ranging from 80 to 200 K. The RE^{3+} co-doping has been found to have a different effect on the thermoluminescence properties of $Sr_3Al_2O_6:Eu^{3+}$ depending on the RE^{3+} ion [45]. The thermoluminescence properties of the $Sr_3Al_2O_6:Eu^{3+}$, RE^{3+} materials should accordingly be affected in a different manner by co-doping.

The following criteria are presently used in judging the effect of RE^{3+} co-doping:
(1) total intensity of the bands in the TL glow curves,
(2) relative intensities of the different TL bands, and
(3) the creation or annihilation of TL bands or modification of TL band temperature.

The TL of $Sr_3Al_2O_6$ doped with 1% Eu^{3+} exhibits the TL pattern which generates a broad peak at -125°C. Addition of Eu^{3+}(1%) in the $Sr_3Al_2O_6:Tb^{3+}$(0.1%) generates well resolved and high intensity isolated TL peak at -124°C. Doping of Sm^{3+} (0.1%) along with Eu^{3+}(1%) to the host matrix resolves the two peaks with high intensity at -130°C and -143°C. Changing the RE^{3+} co-dopant to the adjacent element in the rare earth series affects significantly the thermoluminescence intensity and even the position of the glow curve maximum. The physical effect seemed to quenching the traps since the Tb^{3+} ions suppressed the thermoluminescence.

The quenching of the thermoluminescence by Tb^{3+} was concluded to be due to the presence of Tb^{4+} that results in removal/destruction of TL intensity at -125°C. As far as the total intensity of the bands in the TL glow curves are concerned, the $Sr_3Al_2O_6:Eu^{3+}$ materials co-doped with Tb^{3+} strongly suppresses the TL intensity, by about 60%,

compared to that of $Sr_3Al_2O_6:Eu^{3+}$. The Tb^{3+} doping has a severe suppressing effect, and the TL band positions remain practically the same as without Tb^{3+}. Tb^{3+} ions do not produce any new traps in comparison to the non-co-doped material.

The co-doping of Sm^{3+} creates new traps. The Sm^{3+} ion has, however, a beneficial effect by shifting TL peak temperature higher when compared to the basic $Sr_3Al_2O_6:Eu^{3+}$ material. Co-doping the $Sr_3Al_2O_6:Eu^{3+}$ with Mg^{2+} does not change the peak position much, but increases the TL intensity of the peak by small amount.

The addition of Er^{3+} in the $Sr_3Al_2O_6:Eu^{3+}$ causes the reduction in the TL intensity without changing the peak position. Thus from the above studies it is clear that, after addition of co-dopant in the system does not able to create the traps near room temperature which are responsible for phosphorescence.

Hence in the $Sr_3Al_2O_6$ system no phosphorescence was observed when doped with rare earths.

----------x----------x----------x----------

5.6. References

[1] H. C. Froelich U. S. Pat. 2,392,814 (Jan15, 1946).

[2] Belgian Pat. 1,347,459 (Nov. 18, 1963).

[3] F. C. Palilla A. K. Levin, M. R. Tomkus, J. Electrochem. Soc. **115** (1968) 642.

[4] N. A. Sirazhiddinov, P. A. Arifov., Russ. J. Inorg. Chem. **16** (1971) 40.

[5] T. Matsuzawa, Y. Aoki, N. Takeuchi, Y. Murayama, J. Electrochem. Soc. (8) **143** (1996) 2670.

[6] Morito Akiyama, Chao-Nan Xu, Kazuhiro Nonaka, and Tadahiko Watanabe, Applied Physics Letters, Vol .73, No.21, (1998).

[7] R.C. Powell, G. Blasse, in Luminescence and Energy Transfer, Vol. 42 (Ed.:J.D.Dunitz), Springer-Verlag, Berlin, 1980, pp.43.

[8] F.E. Auzel, Proceedings of the IEEE 1973, 61, 758.

[9] G. Blasse, *Materials Chemistry and Physics* **1987**, *16*, 201.

[10] Xiaoming Teng, Weidong Zhuang, Yunsheng Hu, Chunlei Zhao, Huaqiang He, Xiaowei Huang, Journal of Alloys and Compounds 458 (2008) 446.

[11] Deng Chao-Yong, He Da-Wei, Zhuang Wei-Dong, Wang Yong-Sheng, Kang Kai and Huang Xiao-Wei, Chinese Physics, Vol 13 No 4 (2004) 473.

[12] H. Kawai, T. Abe, T. Hoshina, Japanese Journal of Applied Physics, Vol. 20, 2 (1981) 313.

[13] M.V. Nazarov, J.H. Kang, D.Y. Jeon, E.-J. Popovici, L. Muresan, B.S. Tsukerblat, Solid State Communications 133 (2005) 183.

[14] R.P. Rao and D.R. Rao, Bull. Mater. Sci., Vol. 5, 1 (1983) 29.

[15] D Haranath, Pooja Sharma and Harish Chander, J. Phys. D: Appl. Phys. 38 (2005) 371.

[16] H.S. Jeon, S.K. Kim, H.L. Park, G.C. Kim, J.H. Bang, B. Lee, Solid State Communications, 120 (2001) 221.

[17] Miroslaw Batentschuk, Andres Osveta, Gabi Schierning, Andreas Klier, J-urgen Schneider, Albrecht Winnacker, Radiation Measurements ( ) –

[18] G. Blasse, B.C. Grabmaier, Luminescent Materials, Springer-Verlag, Berlin, 1994.

[19] A.S. Marfunin, Spectroscopy, Luminescence and Radiation Centers in Minerals, Springer-Verlag, Berlin, 1979.

[20] T. Schweizer, T. Jensen, E. Heumann, and G. Huber, Opt.Commun. **118**, 557 (1995).

[21] R. M. Ranson, E. Evangelou, and C. B. Thomas, Appl. Phys. Lett. **72**, 2663 (1998).

[22] H. Yuan, W. M. Dennis, L. Lu, W. Jia, H. Liu, and W. M. Yen, in *Proceedings of the Sixth International Conference on Luminescent Materials*, Paris, 1997, edited by R. Ronda and T. Welker, Electrochem. Soc. Proc., Vol. 97-29 (The Electrochemical Society, Inc., Pennington, NJ, 1998), p. 206.

[23] M. Raukas, "Luminescence efficiency and electronic properties of cerium doped insulating oxides," thesis (The University of Georgia, 1997).

[24] B. M. Tissue, L. Lu, W. Jia, and W. M. Yen, J. Cryst. Growth **109**, 323 (1991).

[25] Shionoya S, Yen W M, Hase T, Kamiya S, Nakazawa E, Narita K, Ohno K,Weber M and Yamamoto H 2000 Phosphor Handbook (New York: CRC Press) p323.

[26] C.K. Chang, D.L. Mao, J.F. Shen, C.L. Feng, J. Alloys Compd. 348 (2003) 224.

[27] C.K. Chang, L. Jiang, D.L. Mao, C.L. Feng, Ceram. Int. 30 (2004) 285.

[28] A. Nag, T.R.N. Kutty, Mater. Res. Bull. 39 (2004) 331.

[29] A. Nag, T.R.N. Kutty, J. Alloys Compd. 354 (2003) 221–231.

[30] W. Minquan, D. Wang, L. Guanglie, Mater. Sci. Eng. B 57 (1998) 18.

[31] M. Marchal, E. Cordoncillo, P. Escribano, M. Vallet-Regi, J.B. carda, Key Eng. Mater. 206–213 (2002) 1207–1210.

[32] MoritoAkiyama ,Chao-Nan Xu,MasanoriTaira, KazuhiroNonaka and Tadahiko Watanabe, Philosophical Magazine Letters, 1999, VOL. 79, 9, 735.

[33] Z. Pei, Q. Su, J. Zhang, J. Alloys Comp. 198 (1993) 51.

[34] T. Zhang, Q. Su, S.Wang, Chin. J. Lumin. 20 (1999) 170–175 (in Chinese).

[35] H. Yamamoto, T. Matsuzawa, J. Lumin. 72–74 (1997) 287–289.

[36] X. Teng,W. Zhuang, C. Zhao, H. Zhao, Y. Fang, Y. Chang, Y. Sun, J. Rare Earths 22 (3) (2004) 412–416 (in Chinese).

[37] J. Niittykoski, T. Aitasalo, J. H¨ols¨a, H. Jungner, M. Lastusaari, M. Parkkinen, M. Tukia, J. Alloys. Compd. 374 (2004) 108–111.

[38] Y. Li, Rare earth 19 (3) (1998) 68–72.

[39] D. Wang, M. Wang, Mater. Sci. Eng. 16 (4) (1998) 40–43.

[40] N. Abanti, T.R.N. Kutty, J. Alloys. Compd. 354 (2003) 221–231.

[41] I.-C. Chen, T.-M. Chen, J. Mater. Res. 16 (3) (2001) 644–651.

[42] Garlick G F J 1949 *Luminescent Materials* (Oxford: Oxford University Press) p 73

[43] Pallavi Page, Rahul Ghildiyal, K.V.R.Murthy, V.Natarajan and B.C.Bhatt, In the Proceedings volume of International Confernece of Luminescence Society, ICLA-08, New Delhi.

[44] Yun Liu and Chao-Nan Xu, J. Phys. Chem. B 107 (2003) 3991.

[45] T. Aitasalo, P. Dere´n, J. Hölsä, H. Jungner, J.C. Krupa, M. Lastusaari, J. Legendziewicz, J. Niittykoski, W. Strek, J. Solid State Chem. 171 (2003) 114.